Incorporating Control Strategies into the Optimization of Synchronous AC Machines: A Comparison of Methodologies

Mohammad Hossain Mohammadi, Rodrigo C. P. Silva and David A. Lowther

McGill University, Department of Electrical and Computer Engineering, Montreal QC, Canada

This paper tests an optimization methodology which emulates a control strategy for synchronous AC machines. Using a conflict measure of different performances, such as average torque and torque ripple, a quantitative validation and comparison is presented for two examples using finite element analysis: an interior permanent magnet machine and a synchronous reluctance machine.

***Index Terms*— AC machines, design optimization, finite element analysis, machine vector control, torque.**

I. Introduction

In recent years, the design of synchronous AC machines, like Synchronous Reluctance (SyR) and Interior Permanent Magnet (IPM) motors, has undergone significant improvement through optimization research. As discussed in previous works [1], [2], [3], both discrete (e.g. number of slots, poles) or continuous (e.g. the width of the tooth/flux barrier) design variables are considered in the initial sizing of an electric machine.

During an optimization procedure, however, various performance indices (e.g. average torque, torque ripple) are required and, generally evaluated using Finite Element Analysis (FEA). Often, each performance depends on pseudo-variables (e.g. for an applied control strategy) which adds more complexity to the existing optimization formulation. For instance, the Maximum-Torque-Per-Ampere (MTPA) control strategy of a synchronous AC machine defined by (1) finds the advance angle, γ, which maximizes the average torque, T_{avg}, for a fixed current magnitude below the base speed operation.

$$\begin{aligned} &\max. \quad T_{avg}(\gamma) \\ &\text{s.t.} \quad \gamma_l \leq \gamma \leq \gamma_u \end{aligned} \tag{1}$$

Mohammadi et al. [4] proposed a general methodology to incorporate a motor control strategy, e.g. MTPA in (1), as a sub-problem within an optimization framework. Using one γ value for all rotor designs may not yield accurate results due to the *dq*-inductance variation [3]. Moreover, their results demonstrated an improvement in the torque ripple, T_{rip}, as well as in T_{avg} when the MTPA strategy was used for a V-shaped IPM motor. Despite this positive outcome, it was noticed that the direct approach (i.e. a simpler optimization without the MTPA strategy and γ added as an additional design variable) was superior to the proposed methodology for the 3-barrier SyR example. Both these methodologies are explained in Section II.

To explain these results, it was hypothesized that T_{avg} and T_{rip} were not in conflict near the SyR's initial design; i.e. minimizing T_{rip} implies maximizing T_{avg} which signifies 0% conflict. In summary, a 100% conflict means that one performance improves at the expense of another, while 0% signifies total harmony, that is, an improvement in T_{avg} implies an improvement in T_{rip}. Any midway value implies a non-uniform trade-off relationship between the performances over the design space. Hence, the SyR's outcome shows that minimizing T_{rip} in terms of γ would incorporate the MTPA control strategy automatically. It also suggests that two performances can be in harmony for some design regions which then permits the use of a computationally cheaper methodology instead.

Therefore, in this paper, we extend the analysis presented in [4] by quantitatively measuring the conflict between T_{avg} and T_{rip} using [2] and testing the proposed methodology for different initial points in the design space. The goal is to explain why and when the direct methodology works, which, in turn, would help to save computational time. Results in both IPM and SyR optimization related problems show that by using conflict analysis, the optimization performance can be predicted.

II. Methodology

Typically, the design optimization of any electrical machine involves two sets of variables; design variables, $\boldsymbol{x}$, that are set by the designer, and control variables, $\boldsymbol{c}$, which depend on the employed control strategy. In a direct optimization framework, both $\boldsymbol{x}$ and $\boldsymbol{c}$ are treated together as lumped variables to the global optimization as shown in Fig. 1 (a). Conversely in Fig. 1 (b), a control strategy emulator (CSE) computes the optimal control parameters by solving a unidimensional problem such as (1). This becomes important during normal operation, because $\boldsymbol{c}$ may assume values which are completely different from the ones found by the optimization method. In this work, the Golden search method with parabolic interpolation (GSM) described in [4] and [5] is used as the CSE, due to its derivative-free and surrogate-based nature as well as its superiority over other deterministic methods.

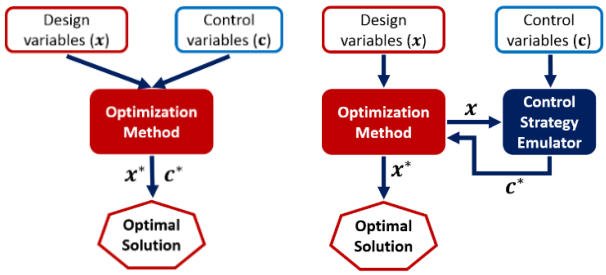

Fig. 1. Motor optimization methodology [4]: (left) direct, (right) proposed.

For each initial point, the conflict between the T_{avg} and T_{rip} performances are calculated using the methodology introduced in [2]. A ranking system is then used to calculate the conflict for each initial point, $\boldsymbol{x_0}$, as explained below. A Latin Hypercube Sampling around $\boldsymbol{x_0}$ is performed within given bounds in order to obtain the set of local samples, $\boldsymbol{X} = \{\boldsymbol{x_0^1}, \dots, \boldsymbol{x_0^n}\}$, where n is the total number of local samples. Then, a vector $\boldsymbol{f_i}(\boldsymbol{x_0^i})$, comprised of (T_{avg}, T_{rip}), for each local sample, is constructed to form the set $\boldsymbol{F} = \{\boldsymbol{f_1}, \dots, \boldsymbol{f_n}\}$. The values of T_{avg} and T_{rip} are then replaced by their relative ranks. The lowest value of T_{avg} receives rank 1, the second lowest receives rank 2, and so on. The same process is performed for T_{rip}. Once each local sample is ranked, the conflict between T_{avg} and T_{rip} can be calculated using (2), where, C_{ab} is the conflict level between two performances and is normalized for n samples.

$$\begin{aligned} C'_{ab} &= \sum_{i=1}^{n} |\boldsymbol{R}_{i,T_{avg}} - \boldsymbol{R}_{i,T_{rip}}| \\ C_{ab} &= C'_{ab} / \sum_{i=1}^{n} |2i - n - 1| \end{aligned} \tag{2}$$

III. Problem Statement

Two single-objective problems are formulated in (3) based on the two methodologies presented in Fig. 1, since it is simple to compare the final solutions. Here, T_{rip} is to be minimized as a function of $\boldsymbol{x}$. Also, $\boldsymbol{x}$ must belong to the set of feasible designs, $\mathcal{F}$, and is restricted to the neighborhood of $\boldsymbol{x_0}$. The inequality constraint for T_{avg} only considers nonzero values, i.e. motoring operation. At high conflicts, optimal solutions may no longer achieve improved T_{avg} over the initial design. Note that there is a significant difference between the two formulations in (3). For the direct approach, γ is added as an extra design variable, whereas the proposed approach emulates the MTPA control strategy by finding its optimal γ_{MTPA} to maximize T_{avg} for a given current magnitude and $\boldsymbol{x}$.

Direct approach

$$\begin{aligned} &\min_{x,\gamma} \left(T_{rip}(\boldsymbol{x},\gamma)\right) \\ &\text{s.t. } T_{avg}(\boldsymbol{x},\gamma) \geq 0 \\ &\quad \boldsymbol{x_l} \leq (\boldsymbol{x} \in \mathcal{F}) \leq \boldsymbol{x_u} \end{aligned}$$

MTPA (proposed)

$$\begin{aligned} &\min_{x} \left(T_{rip}(\boldsymbol{x},\gamma_{\text{MTPA}})\right) \\ &\text{s.t. } \gamma_{\text{MTPA}} = \underset{\gamma}{\text{argmax}} \left(T_{avg}(\boldsymbol{x},\gamma)\right) \\ &\quad T_{avg}(\boldsymbol{x},\gamma_{\text{MTPA}}) \geq 0 \\ &\quad \boldsymbol{x_l} \leq (\boldsymbol{x} \in \mathcal{F}) \leq \boldsymbol{x_u} \end{aligned} \tag{3}$$

For each initial point, both problems in (3) are solved to compare their performances using two motor models: a V-shaped IPM and a 3-barrier SyR. The motor cross-sections with labeled design variables $\boldsymbol{x}$ are shown in Fig. 2. Despite their similar stator geometries described in [4] (12 slots, 4 poles, 75 mm stator outer diameter, 34 mm stack length, 40/11 mm rotor outer/inner diameter 0.5 mm airgap thickness, 10 A_{rms}/mm^2 RMS current density), their rotor geometries are different. To ensure feasibility, the IPM's V-shaped layer and the SyR's flux barriers are both constrained inside the rotor as explained in [3] and [4]. The instantaneous torque waveform, T, is computed for a fixed sinusoidal current excitation using transient 2D FEA simulations, which benefit from 4-pole and 3-phase periodicities to reduce computation time. Then, T_{rip} and T_{avg} are post-processed from T using a process similar to that described in [3].

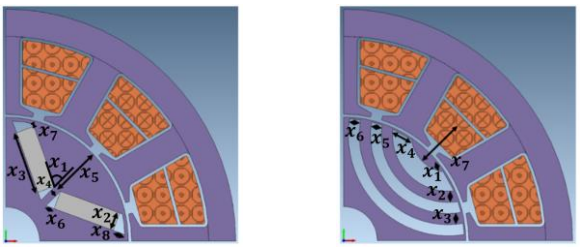

Fig. 2. Motor model cross-sections [4]: (left) IPM, (right) SyR.

IV. Preliminary Results and Future Work

Both optimization problems in (3) are solved for more than 10 initial samples of the IPM and SyR examples. The Pattern Search method was used as the main optimizer, since it can handle several design variables as a direct-search method. Table I below presents the three final solutions of each motor in ascending order of the initial point's conflict level. For high conflict designs, the trade-off between T_{avg} and T_{rip} is noticeable for both motors (in red). Also, the MTPA approach generally performs better than the direct method as illustrated in Fig. 3, except for low conflict IPM designs. The direct approach offers a faster alternative for these low conflict points. For the paper's final version, more detailed results and analysis will be presented for both motor case studies. The impact of an optimal SyR design region on the presented analysis using the methodology in [3] will also be investigated.

TABLE I
Final Solutions For Different Initial Points

	Conflict [%]	T_{rip} [%]			T_{avg} [Nm]		
		Init.	Direct	MTPA	Init.	Direct	MTPA
IPM	31.4	80.12	51.97	63.07	1.39	1.44	1.47
	61.0	61.99	34.37	44.87	0.97	1.04	1.18
	90.4	81.42	60.39	24.91	0.78	0.34	0.46
SyR	31.2	63.27	28.38	23.71	0.74	0.50	0.77
	68.0	29.17	115.17	11.65	0.82	0.17	0.83
	99.6	79.57	29.84	20.03	0.77	0.28	0.54

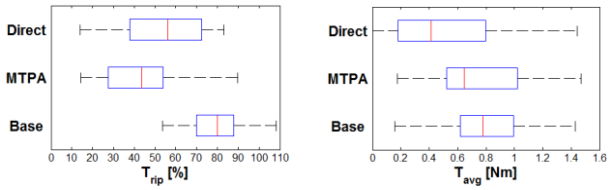

Fig. 3. Boxplots for IPM: (left) torque ripple, (right) average torque.

References

[1] G. Pellegrino, F. Cupertino, and C. Gerada, "Automatic Design of Synchronous Reluctance Motors focusing on Barrier Shape Optimization," *IEEE Trans. Ind. Appl.,* vol. 51, no. 2, pp. 1465-1474, Apr. 2015.

[2] A. R. R. Freitas, P. J. Fleming and F. G. Guimarães, "A Non-Parametric Harmony-Based Objective Reduction Method for Many-Objective Optimization," in *IEEE Intl. Conf. on Systems, Man, and Cybernetics*, Manchester, 2013, pp. 651-656.

[3] M. H. Mohammadi, T. Rahman, R. C. P. Silva, M. Li and D. A. Lowther, "A Computationally Efficient Algorithm for Rotor Design Optimization of Synchronous Reluctance Machines," *IEEE Trans. Magn.,* vol. 52, no. 3, Mar. 2016, doi: 10.1109/TMAG.2015.2491306.

[4] M. H. Mohammadi, R. C. P. Silva and D. A. Lowther, "Finding Optimal Performance Indices of Synchronous AC Motors," *IEEE Trans. Magn.,* vol. 53, no. 6, Jun. 2017, doi: 10.1109/TMAG.2017.2662705.

[5] R. P. Brent, *Algorithms for Minimization Without Derivatives*, Prentice-Hall, 1973.